

## Initial stage of oxygen chemisorption on Na/Pt and Na/Cr: An autoionization-electron-spectroscopy study

Fang Xu and Assunta Bonanno

*Dipartimento di Fisica, Università della Calabria, 87036 Arcavacata di Rende, Cosenza, Italy*

(Received 2 May 1994; revised manuscript received 11 July 1994)

The interaction of  $O_2$  with Na-(polycrystalline Pt and Cr) interfaces at room-temperature Na saturation coverage has been studied with projectile- and target-autoionization electron spectroscopy using low-energy  $Ne^+$ -ion impact. Our results show that for both systems oxygen is initially incorporated beneath the Na atoms. For Na/Pt, further deposited oxygen is uniformly distributed on top of the Na layer, whereas for Na/Cr large patches are formed on the surface.

Alkali-metal and oxygen coadsorption on metal and semiconductor surfaces has been studied for many decades both for the basic understanding of the substrate-oxidation-promotion mechanism and for the potential technological applications.<sup>1</sup> A great deal of information regarding the electronic, chemical, structural, and morphological properties of these systems has been obtained by employing various surface-sensitive techniques as photoemission and Auger-electron spectroscopy, low-energy electron diffraction, and electron-energy-loss spectroscopy,<sup>2-6</sup> etc.

In this paper, we report a study on the initial stage of oxygen chemisorption on Na-covered polycrystalline Pt and Cr surfaces using an interesting surface-sensitive technique. Projectile  $Ne\ 2p^4 3s^2$  and target  $Na\ 2p^5 3s^2$  autoionization-electron emission produced by low-energy  $Ne^+$ -ion impact has been used to monitor the surface work function variation and the growth morphology directly. Our results show that for both systems oxygen is initially incorporated beneath the Na atoms. For the Pt substrate, the second oxygen layer grows uniformly on top of the Na whereas for Cr large patches are formed on the surface. We demonstrate that low-energy collisionally excited autoionization spectroscopy can provide unique electronic and morphological information on these systems.

The experiments were performed in an UHV chamber with a base pressure of  $5 \times 10^{-10}$  Torr. Incident on polycrystalline Pt and Cr samples were 700-eV  $Ne^+$  projectile ions at an angle of  $70^\circ$  relative to the surface normal and the total ion current was of the order of  $10^{-8}$  A. To reduce sputtering effects, the beam was set to raster over a large surface area of  $4 \times 4\ mm^2$  and the samples were exposed to the ion beam only during data acquisition (typically less than 1 min). Na/Pt and Na/Cr interfaces were prepared at room temperature by evaporating Na from commercial dispensers until saturation coverage was reached. Spectra were collected either by sequential oxygen exposure or by depositing the desired amount of oxygen directly onto the freshly prepared sample and no difference was observed. The emitted electrons were collected with a hemispherical energy analyzer working at a constant energy resolution of 0.2 eV and its axis was normal to the surface.

In the left panel of Fig. 1 is depicted a set of Ne and Na autoionization electron spectra for the Na/Pt system after ex-

posure to increasing amounts of oxygen. These spectra have been corrected for the analyzer-transmission factor, background subtracted, and normalized to the same height. In the right panel are shown line-shape fittings using Gaussian curves for some typical  $O_2$  coverages. The three main sharp peaks are commonly assigned to the atomic autoionization decays from the  $Ne\ 2p^4(^3P)3s^2\ ^3P$  and  $2p^4(^1D)3s^2\ ^1D$  (labeled as Ne-I and Ne-II in the figure) and from the  $Na\ 2p^5 3s^2\ ^3P$  (labeled as Na) states, respectively.<sup>7,8</sup> The other two small features seen at high exposures (labeled as *a* and *b*) are due to emission from the  $Ne\ 2p^4(^3P)3s3p(^3P)\ ^3D$  and  $Na\ 2p^5 3s3p\ ^4S$  states.<sup>8,9</sup>

According to the molecular-orbital (MO) promotion model,<sup>10</sup> during a close collision between a Ne and a Na atom, the two electrons in the  $4f\sigma$  MO, which is correlated to the  $Ne\ 2p$ , can be promoted to unfilled high-lying levels resulting in the creation of a  $Ne^{2+}\ 2p^4(^1D)$  state. Such a singlet-core configuration can also be converted to a  $^3P$  triplet in the close vicinity of the excitation site.<sup>11</sup> On the other hand, the  $Na\ 2p$  excitation can either be achieved through an *L*-shell vacancy transfer from Ne (Ref. 12) or be directly produced in a secondary symmetric collision between two target Na atoms. When receding from the surface, these excited Ne and Na ions may form autoionizing states by capturing electrons from the valence band of the solid into the outer shells through Auger or resonant neutralization.<sup>7</sup>

Deexcitation of these scattered atoms in vacuum gives rise to the narrow peaks seen in the spectra of Fig. 1. As discussed in detail by Zampieri and Baragiola,<sup>13</sup> unlike the case of atoms in a solid for which all binding energies are referred to the Fermi level  $E_F$ , the electronic energies of a free atom are referred to the vacuum level  $E_{vac}$ , i.e., the kinetic energy  $E_{k0}$  of an electron emitted in an atomic particle is constant with respect to  $E_{vac}$ . The detected electron energy  $E_k$ , which is relative to the  $E_F$  of the sample, is given by  $E_k = E_{k0} + \Phi$ , where  $\Phi$  denotes the sample work function. Therefore, the change in  $E_k$  can be used as a direct measure of the variation of  $\Phi$ , as clearly demonstrated in all previous studies (see Ref. 13 as an example). The so-measured  $\Phi$  is 5.57 eV for clean Pt and 2.70 eV for Na saturated surfaces. It should be pointed out that because of the relatively long lifetime of these autoionizing states ( $\sim 2 \times 10^{-13}$  sec, see Ref. 9), deexcitation events may take place quite far away

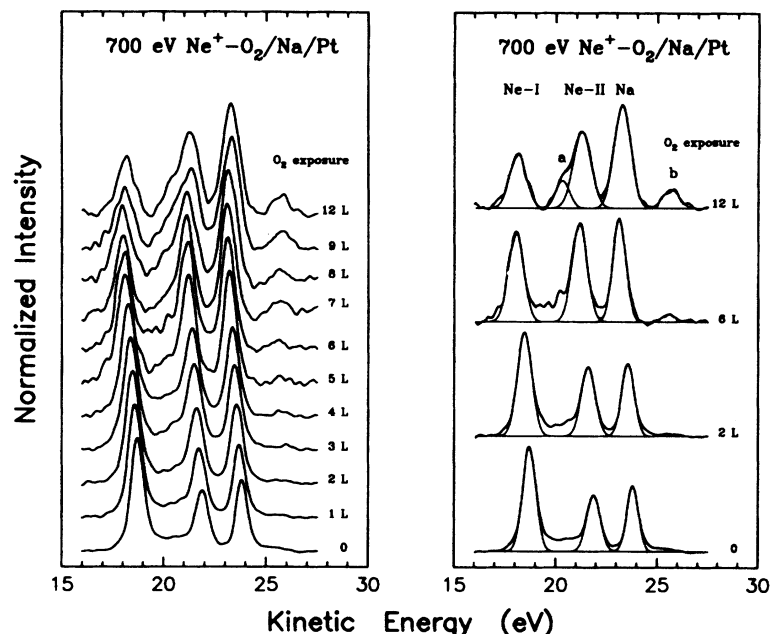


FIG. 1. Left panel: background subtracted Ne and Na autoionization electron spectra obtained by 700-eV Ne<sup>+</sup> impact on Na/Pt at Na saturation coverage upon exposure to increasing amounts of O<sub>2</sub>. Right panel: line-shape fittings using Gaussian curves for some typical O<sub>2</sub> coverages.

from the excitation sites (a few nm) and the work function seen by these atoms is an averaged value. The presence of impurities and the consequent inhomogeneity of the electrostatic potentials at different atomic sites then may cause a broadening of the spectral lines.

The peak energy shift, measured with respect to the clean Pt surface, the total Ne and Na intensities, taken by integrating the areas underneath their spectral features, the full width at half maximum (FWHM) of the Na atomic peak, obtained through line-shape curve fittings and representative also for the behavior of the Ne peaks, and the Na-to-Ne intensity ratio  $\rho$  are plotted in the left panel of Fig. 2 as a function of the oxygen exposure  $\Theta(\text{O}_2)$ . The initial dramatic decrease of both the Ne and Na autoionization peak intensities reflects a great reduction of the surface electron density upon oxidation and a consequent reduction of electron-capture probability in the exit trajectory. The increase of the Ne singlet peak relative to the triplet one seen in Fig. 1 would indicate a continuous decrease of the 3s electron density around the outermost Na sites available for participating to the singlet-to-triplet conversion process, as has been discussed in detail in Ref. 11.

The initial broadening of all the atomic peaks reflects the increasing inhomogeneity of the electronic property of the surface and the subsequent narrowing indicates a gradual flattening of the surface vacuum level. For  $\Theta(\text{O}_2)$  up to 4 L (1 L =  $10^{-6}$  Torr sec), the averaged surface work function decreases continuously whereas the Na-to-Ne intensity ratio remains essentially constant. This suggests that oxygen is initially incorporated underneath the Na atoms. The so-formed Na-O double layer produces a quite large positive surface dipole resulting in a decrease of  $\Phi$ . The nearly same binding energies of their outer *M* shells makes very unlikely any substantial difference in the electron-capture probability, thus the observed constancy of  $\rho$  can be explained as due to the occurrence of practically all the excitation events at the surface. Indeed, the room-temperature saturation coverage of

a Na layer deposited on Pt is only about 1 ML, as judged by the Na-to-Ne intensity ratio (see Ref. 14 for a detailed discussion), and collisions involving O and Pt atoms do not produce 2*p* electron excitation in either Ne or Na.

As more oxygen is deposited, a drastic increase of  $\rho$  and a substantial broadening of all the atomic peaks can be clearly seen in the spectra of Fig. 1 and in the plots of Fig. 2. Starting from  $\Theta(\text{O}_2) = 6-7$  L, the surface work function also gradually increases. All together these results suggest that the deposited oxygen now is adsorbed on top of the Na layer. Indeed, the presence of oxygen on the surface, on one hand, can decrease the dipole strength causing a backshift of  $\Phi$ , and on the other hand, can efficiently shadow the underlying Na atoms greatly reducing the Ne-Na asymmetric collision events, and thus the Ne intensity. The symmetric collisions between the target Na atoms, however, are much less influenced since the energy transfers between Ne-O and O-Na can be quite substantial and the threshold energy for the Na 2*p* excitation in symmetric collisions is expected to be only around 300 eV.<sup>15</sup> The fact that only one single component is observed for all atomic peaks through all  $\Theta(\text{O}_2)$  suggests a quite uniform distribution of oxygen both beneath and above the Na layer. The increase of the Na-to-Ne intensity ratio and the simultaneous decrease of the surface work function for O<sub>2</sub> exposure between 4 and 7 L may be an indication that the second oxygen layer starts to form on the Na surface before the completion of the first one beneath Na.

The situation for the O<sub>2</sub> exposure of the Na/Cr system presents both similarities and differences with respect to Na/Pt. In Fig. 3 we show a set of Ne and Na autoionization spectra and some typical line-shape fittings. The results of detailed analysis are plotted in the right panel of Fig. 2. For coverage up to 10 L, oxygen is incorporated beneath the first Na layer, just as in the case of Na/Pt. The decrease of the Na-to-Ne intensity ratio can be attributed to the fact that Na forms multilayers on the Cr surface (the initial  $\rho$  for clean Na/Cr is larger than that for Na/Pt) and the contribution of

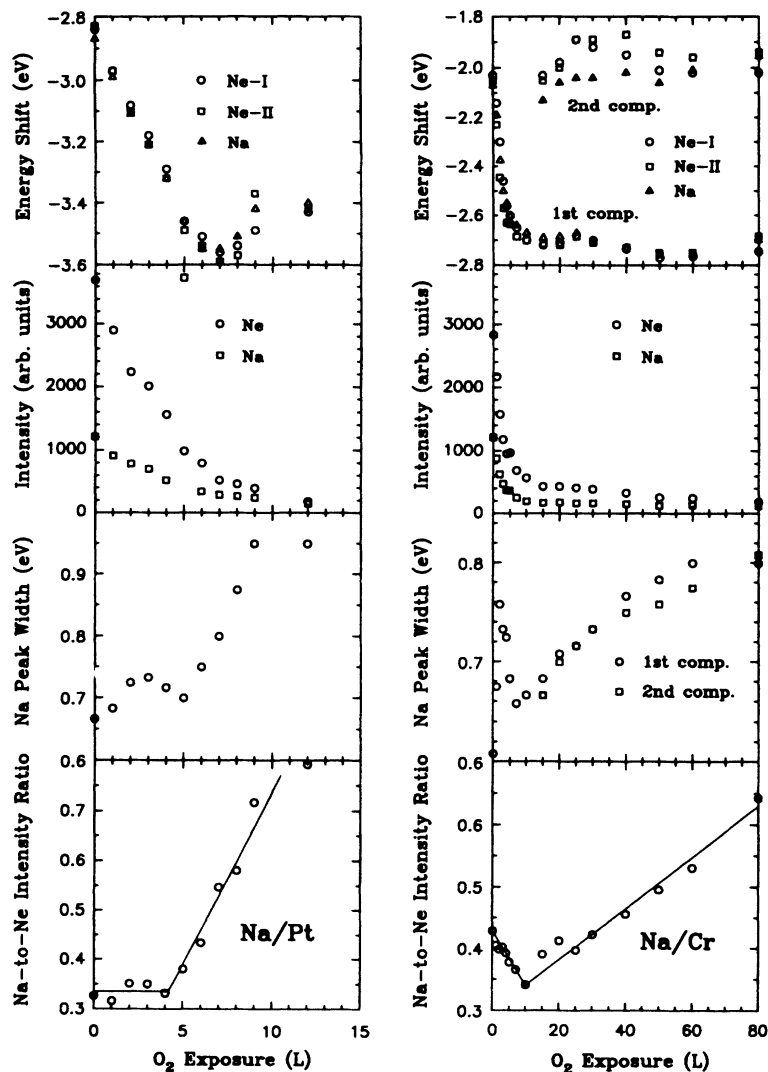


FIG. 2. Peak energy shift, Ne and Na intensities, FWHM of the Na  $2p^5 3s^2$  line, and the ratio between the total intensities of Na and Ne as a function of O<sub>2</sub> exposure for Na/Pt (left panel) and Na/Cr (right panel) systems.

Na-Na collisions is more important. Indeed, the presence of oxygen sandwiched between two Na layers does not influence the Ne-Na collision events occurring mainly at the surface but can reduce the number of Na-Na ones taking place below the surface.

The most striking result for this interface is the appearance and the gradual growth of a new component on the high-energy side of all the atomic peaks when the surface work function reaches its minimum. These components cannot be attributed to other atomic transitions since they are not observed for Na/Pt. Instead, they would suggest the formation of large patches with very different electrostatic potentials. The increase of the ratio between the total Na and Ne intensities with  $\Theta(\text{O}_2)$  indicates the presence of oxygen on the surface. We also note that this ratio increases faster for the second components of Na and Ne than for the first ones, though an accurate evaluation is complicated by the use of only a single component for the Ne  $2p^4(^3P)3s3p(^3P)^3D$  peak for high coverages. The electrons emitted during deexcitation close to these patches correspond to the second components with higher  $E_k$  and those emitted near the uncovered surface area correspond to the first components with lower  $E_k$ .

For alkali-metal coverage higher than a critical value (corresponding to the surface work-function minimum), the initial subsurface and the subsequent on-top oxygen chemisorption on alkali adlayers have been invoked in many previous studies<sup>2-5</sup> to interpret the exposure dependence of the work-function changes, but these conclusions were not based on the direct spectroscopic evidence. Argile and Rhead<sup>5</sup> explicitly stated that they used the terms "underneath" and "on-top" adsorption to indicate the direction of the surface dipole but not to describe the real spatial atomic location for O<sub>2</sub> chemisorption on K/Cu(111). Papageorgopoulos<sup>4</sup> suggested that the second oxygen layer adsorbed on Cs-covered Cu(100) is only weakly bound and can be easily removed by gentle heating. Based on the observation that the electron energy loss decreases continuously with oxygen coverage for Cs/Cu(111) but remains essentially constant for Na/Cu(111), Lindgren and Wallden<sup>2</sup> argued that the oxygen distribution is uniform in the first case whereas clustering may occur in the latter system. Surnev, Ramgelov, and Kiskinova<sup>3</sup> observed a shoulder in the retarding potential  $I$ - $V$  curves for oxygen chemisorption on K-covered Ru(100) with potassium coverage exceeding 0.12 and attributed it to the formation of patches with different surface work functions. However,

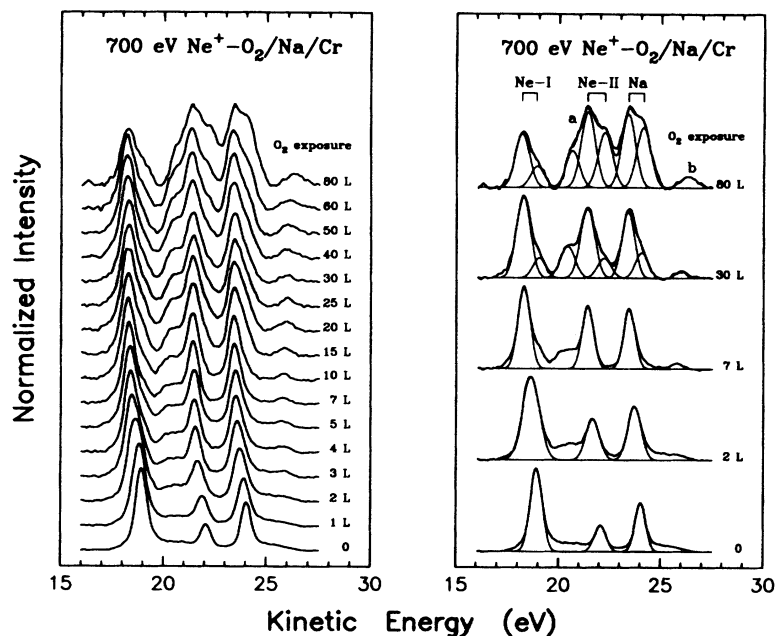


FIG. 3. Left panel: background subtracted Ne and Na autoionization electron spectra obtained by 700-eV  $\text{Ne}^+$  impact on Na/Cr at Na saturation coverage upon exposure to increasing amounts of  $\text{O}_2$ . Right panel: line-shape fittings using Gaussian curves for some typical  $\text{O}_2$  coverages.

these measurements did not allow a quantitative estimate of the difference of  $\Phi$  of these patches.

In conclusion, we have demonstrated that the collisionally excited projectile- and target-autoionization spectroscopy can provide direct information regarding the surface work-function variation on a nm scale of lateral extension and the growth morphology. In particular, the Na-to-Ne intensity ratio clearly indicates that for both Na/Pt and Na/Cr, oxygen is initially incorporated underneath and then grows on top of

the Na adlayer. We have shown that for Na/Pt the distribution of oxygen on the surface is laterally uniform, while for Na/Cr large patches are formed. Further, we have reported the quantitative measurements of the surface electrostatic potentials of these patches for the latter systems.

We thank V. Fabio and E. Li Preti for technical assistance. The Laboratory is also affiliated with Consorzio Interuniversitario Nazionale della Fisica della Materia.

<sup>1</sup> *Physics and Chemistry of Alkali Metal Adsorption*, edited by H. P. Bonzel, A. M. Bradshaw, and G. Ertl (Elsevier, Amsterdam, 1989), and references therein.

<sup>2</sup> S. A. Lindgren and L. Wallden, *Phys. Rev. B* **22**, 5967 (1980).

<sup>3</sup> L. Surnev, G. Ramgelov, and M. Kiskinova, *Surf. Sci.* **179**, 283 (1987).

<sup>4</sup> C. A. Papageorgopoulos, *Phys. Rev. B* **25**, 3740 (1982).

<sup>5</sup> C. Argile and G. E. Rhead, *Surf. Sci.* **279**, 244 (1992).

<sup>6</sup> G. Pirug, H. P. Bonzel, and G. Broden, *Surf. Sci.* **122**, 1 (1982).

<sup>7</sup> G. E. Zampieri and R. A. Baragiola, *Surf. Sci.* **114**, L15 (1982).

<sup>8</sup> N. Andersen and J. O. Olsen, *J. Phys. B* **10**, L719 (1977).

<sup>9</sup> O. I. Zatsarinny and L. A. Bandurina, *J. Phys. B* **26**, 3765 (1993).

<sup>10</sup> M. Barat and W. Lichten, *Phys. Rev. A* **6**, 211 (1972).

<sup>11</sup> F. Xu, R. A. Baragiola, A. Bonanno, P. Zoccali, M. Camarca, and A. Oliva, *Phys. Rev. Lett.* **72**, 4041 (1994).

<sup>12</sup> J. O. Olsen, T. Andersen, M. Barat, Ch. Courbin-Gaussorgues, V. Sidis, J. Pommier, J. Agusti, N. Andersen, and A. Russek, *Phys. Rev. A* **19**, 1457 (1979).

<sup>13</sup> G. E. Zampieri and R. A. Baragiola, *Phys. Rev. B* **29**, 1480 (1984).

<sup>14</sup> P. Zoccali, A. Bonanno, M. Camarca, A. Oliva, and F. Xu, *Phys. Rev. B* (to be published).

<sup>15</sup> The threshold energy for  $2p$  electron excitation in symmetric collisions decreases from  $\sim 1450$  eV for Si-Si to  $\sim 800$  eV for Al-Al, and to  $\sim 450$  eV for Mg-Mg. See N. Mandarino, P. Zoccali, A. Oliva, M. Camarca, A. Bonanno, and F. Xu, *Phys. Rev. A* **48**, 2828 (1993).